Precise Direct Position Estimation: Validation Experiments

Shuo Tang, Haoqing Li, Helena Calatrava, Pau Closas
Northeastern University
Dept. of Electrical & Computer Eng.
Boston, MA (USA)
{tang.shu, li.haoq, calatrava.h, closas}@northeastern.edu

2023 IEEE/ION Position, Location and Navigation Symposium (PLANS) | 978-1-6654-1772-3/23/$31.00 ©2023 IEEE | DOI: 10.1109/PLANS53410.2023.10140046

***Abstract*—Direct position estimation is an alternative GNSS positioning method, which parameterizes the received satellite signals as a function of the target dynamics and solves the position, velocity, and time (PVT) quantities directly from the raw signal, as opposed to using observables. It is also recognized as a one-step positioning method, in contrast to the traditional two-step GNSS positioning method which first estimates the observables and then estimate PVT through those intermediate quantities. It has been shown that DPE outperforms the two-step method in low-SNR scenarios, where the early combination of the signals improve the receiver sensitivity and its exploitation of weak signals. This paper improves the existing DPE approach by modeling the carrier phase components in terms of the position of the receiver. In this new framework, termed Precise DPE (PDPE), a new maximum likelihood estimator is derived based on the proposed signal model. This article present the first results of PDPE using a real raw GNSS signal dataset, which is used to compare PDPE performance against DPE and two-step solutions. Results show that PDPE provides improved precision compared to DPE and, additionally, outperforms the two-step method in precision and sensitivity.**

***Index Terms*—GNSS, direct positioning, precise positioning, maximum likelihood estimator**

I. Introduction

Global navigation satellite system (GNSS) provides positioning, navigation and timing solutions by utilizing transmitted signals from satellites. The common GNSS positioning method is to estimate the observables, e.g. pseudorange, Doppler shift and carrier phase, and determine the position through these observables. This traditional method and its advanced techniques for improving positioning performance, such as dual frequencies, real-time kinematics and precise point positioning, have been thoroughly described in many famous GNSS textbooks [1]–[5]. Specially, detailed software configurations and practical algorithms are discussed in [6], which helps the real-world GNSS receiver design on the Global position system (GPS) and Galileo. However, the GNSS positioning performance could be extremely mitigated in unfavorable environments [7], [8], such as indoor scenarios, multipath propagation, signal jamming, poor satellite geometry and high dynamics target. High-sensitivity (HS) GNSS receivers usually perform better in these harsh environments. For example, long coherent integration time for signal acquisition is designed to improve the capability of the receiver for leveraging weak signals [1], [9].

Direct position estimation (DPE) is such a novel design of a HS GNSS receiver. It computes the position, velocity and time (PVT) solution by fusing the signals from visible satellites at an early stage of processing and thus improves the sensitivity of receiver. The DPE method directly use the received signal to estimate the PVT solution without measuring some intermediate quantities, in contrast to the traditional two-step (2SP) method, which first estimates the observables for each satellite and then use these observables to find the optimal PVT solution usually by Least Square (LS) method. As a HS GNSS receiver technique, the DPE approach has great tolerance of extreme environments. It has been shown that both 2SP and DPE approaches lead to an asymptotically unbiased and precise positioning result with large data record, while the bias and variance of the DPE positioning could be much lower than the ones of 2SP method [10]. From the perspective of estimation error bounds, one could show that the DPE approach outperforms the 2SP approach by comparing their Cramér-Rao bounds [11], [12]. Besides, when the a priori information is exploited, the Bayesian bound (e.g. Ziv-Zakai bounds) can help predict the maximum likelihood (ML) estimator performance under different carrier-to-noise density (C/N_0) levels [13], [14] and DPE has a robust behavior than 2SP does in the sense that it can operate at lower carrier-to-noise density (C/N_0) value.

In GNSS DPE approach, the received signal model should be formulated as a function of the dynamics of the receiver. This model and the corresponding ML estimator have been explicitly clarified in [15]. However, most of the existing works on DPE receivers consider the received satellite signal model as a pure pseudo-random noise (PRN) code model without a carrier-phase component which depends on the target PVT parameters. The assumption is convenient for the simulation implementation, but could reject the high-precision potential of DPE method, since the carrier phase is obviously more sensitive to the dynamics (e.g. position of the receiver), compared to the chip delay of the C/A code. Besides, the previous work on DPE verifies their result on the simulated satellite signal instead of signals from real-world receivers. In this paper we propose the so-called Precise DPE (PDPE) approach and connect it to the real-world GNSS receiver and

This work has been partially supported by the National Science Foundation under Award ECCS-1845833.

signal processing design through the leverage of carrier-phase parameters.

The rest of this paper is organized as following. In Section II, we will review the DPE model and ML estimator of the previous work. Then we will introduce the received signal model for PDPE and develop a new ML estimator based on that in Section III. In Section IV, we will process the popular dataset sampled from the common real-world GNSS receiver and exploit PDPE approach developed in this paper. The positioning performance among 2SP, DPE and PDPE will be compared and some conclusion will be drawn in Section V based on the experiment results.

II. REVIEW OF DPE APPROACH

As described in [1] and [15], an antenna receives the GNSS signal as a summation of signals from its visible satellites. Each transmission signal has a well-known structure, which includes the time-delay and Doppler shift effects. The distinctive modeling from DPE perspective is that those observables can be modeled by their physical relation with the target states and thus the received signal can be expressed as the function of the target dynamics. For example, the pseudorange, computed as $\rho_i = c\tau_i$ with c being speed of light constant, is modeled as

$$\rho_i = \varrho_i(\boldsymbol{\theta}) + c(\delta t - \delta t_i) + \epsilon_i, \tag{1}$$

with the following definitions:

- $\varrho_i(\boldsymbol{\theta})$ geometric distance $||\boldsymbol{r}_i - \boldsymbol{\theta}||$ between the i-th satellite, located at $\boldsymbol{r}_i = (r_{x,i}, r_{y,i}, r_{z,i})^\top$, and the receiver, whose position $\boldsymbol{\theta} = (\theta_x, \theta_y, \theta_z)^\top$ is to be estimated;
- c speed of light;
- δt the unsolved receiver clock bias with respect to GNSS time;
- δt_i the i-th satellite clock bias with respect to GNSS time given by the ephemeris;
- ϵ_i errors term including ephemeris errors, relativistic effects, etc.

For neat notation, the tropospheric delay ΔT_i, ionospheric delay ΔI_i and multipath effect are ignored in the pseudorange model [5, Ch. 21]. The Doppler shift is modeled as

$$f_{d,i} = -(\boldsymbol{v}_i - \boldsymbol{v})^\top \boldsymbol{u}_i (1 + \dot{\delta t}) \frac{f_c}{c}, \tag{2}$$

where $\boldsymbol{v}_i = (v_{x,i}, v_{y,i}, v_{z,i})^\top$ is the velocity vector of the i-th satellite, $\boldsymbol{v} = (v_x, v_y, v_z)^\top$ is the velocity of the receiver, $\dot{\delta t}$ is the clock shift of the receiver, $\boldsymbol{u}_i$ denotes the unit vector from the receiver pointing to the i-th satellite as shown below

$$\boldsymbol{u}_i = \frac{\boldsymbol{r}_i - \boldsymbol{\theta}}{||\boldsymbol{r}_i - \boldsymbol{\theta}||}, \tag{3}$$

where $||\cdot||$ denotes the 2-norm or Euclidean norm of the vector and f_c denotes the carrier-wave frequency of the received GNSS signal.

Hence, if we consider the the position $\boldsymbol{\theta}$, velocity $\boldsymbol{v}$, clock offset δt, and clock rate $\dot{\delta t}$ as the dynamics of the receiver and concatenate all variables of interest together, e.g., $\boldsymbol{\kappa} = (\boldsymbol{\theta}^\top, \delta t, \boldsymbol{v}^\top, \dot{\delta t})^\top$, the mixed signal model in complex band can be parameterized as

$$x(t) = \sum_{i=1}^{M} a_i s_i(t - \tau_i(\boldsymbol{\kappa})) \exp(j2\pi f_{d,i}(\boldsymbol{\kappa})t) + n(t), \tag{4}$$

where M is the number of satellites the receiver has in view, the subindex $i \in \{1, 2, \cdots, M\}$ denotes each satellite, a is the complex amplitude with its phase being the so-called carrier-phase component $\varphi_i = \angle a_i$, $s(t)$ is the navigation signal spread through PRN code, τ is the time-delay from the satellite to the receiver, f_d is the Doppler-shift, and $n(t) \sim \mathcal{N}(0, \sigma_n^2)$ denotes a complex additive white Gaussian noise (AWGN) process which includes unmodeled terms besides line-of-sight (LOS) signals.

Assuming that $\boldsymbol{x} \in \mathbb{C}^{K\times 1}$ denotes the K-samples vector of the received signals, the ML solution for maximizing the likelihood of this $\boldsymbol{x}$ is equivalent to minimizing the following cost function [5, Ch. 21]:

$$J(\boldsymbol{a}, \boldsymbol{\kappa}) = ||\boldsymbol{x} - \boldsymbol{C}(\boldsymbol{\kappa})\boldsymbol{a}||^2, \tag{5}$$

where $\boldsymbol{C} \in \mathbb{C}^{K\times M}$ denotes a matrix of local replicas whose columns are local replica sequences of K samples generated for each satellite as shown below

$$\boldsymbol{C}(\boldsymbol{\kappa}) = (\boldsymbol{c}_1, \boldsymbol{c}_2, \cdots, \boldsymbol{c}_M), \tag{6}$$

where

$$\boldsymbol{c}_i = \begin{bmatrix} s_i\big(T_s - \tau_i(\boldsymbol{\kappa})\big) \exp\left(-j2\pi f_{d,i}(\boldsymbol{\kappa}) T_s\right) \\ s_i\big(2T_s - \tau_i(\boldsymbol{\kappa})\big) \exp\left(-j2\pi f_{d,i}(\boldsymbol{\kappa}) 2T_s\right) \\ \vdots \\ s_i\big(KT_s - \tau_i(\boldsymbol{\kappa})\big) \exp\left(-j2\pi f_{d,i}(\boldsymbol{\kappa}) KT_s\right) \end{bmatrix}, \tag{7}$$

and $\boldsymbol{a} = (a_1, a_2, \cdots, a_M)^\top \in \mathbb{C}^{M\times 1}$ is the vector of the complex amplitude of each satellite. Then following the derivation from [5, Ch. 21], the ML estimator of $\boldsymbol{\kappa}$ is

$$\begin{aligned} \hat{\boldsymbol{\kappa}} &= \arg\max_{\boldsymbol{\kappa}} \left\{ \sum_{i=1}^{M} |\boldsymbol{x}^H \boldsymbol{c}_i(\boldsymbol{\kappa})|^2 \right\} \\ &= \Lambda_{\text{DPE}}(\boldsymbol{a}, \boldsymbol{\kappa}) \ , \end{aligned} \tag{8}$$

which can also be interpreted as the non-coherent combination of the cross-ambiguity functions (CAF) from the M satellites in such a way that the cost function (8) is maximized.

The optimization performance of (8) will directly affect the precision, accuracy and time cost of the estimation and thus play a great role in DPE implementation. There exists a set of useful optimization tools, such as brute-force grid search, gradient-based method and random search, which have deeply discussed in many fields and applications. From the DPE perspective, for example, an open-source grid-dependent DPE receiver prototype is designed to improve the computational and localization performance by parallelizing computational structure [16]. Some works (e.g. [11] and [5, Ch. 21]) leverage the Accelerated Random Search (ARS) [17] to solve the optimization problem. The following work and experiments

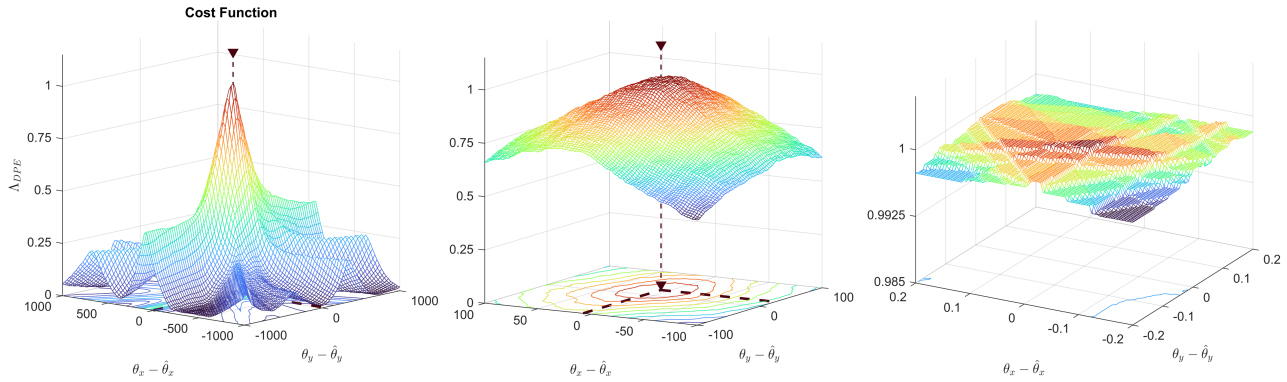

(a) DPE

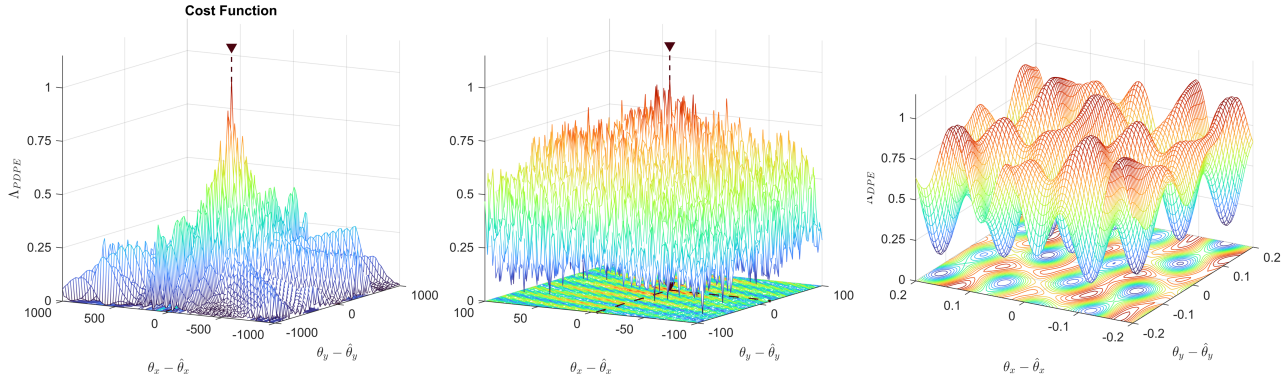

(b) PDPE

Fig. 1. Representation of (a) DPE and (b) PDPE cost functions over a 1000×1000 m^2 area (left), on a zoomed 100×100 m^2 area over the same function range (middle), and a continuously zoomed 0.2×0.2 m^2 area around the true position.

will also use the ARS approach and we will further discuss the choice in the experiment.

III. DPE WITH CARRIER PHASE

In this section, we propose the PDPE approach by relating the carrier phase in the signal model to the receiver dynamics. Then based on this received signal model, we will derive a new ML estimator for receiver dynamics.

One may notice that the received signal model (4) encompasses the carrier phase information in its complex amplitude a_i. In fact, the carrier phase, which is interpreted as the phase change caused by the signal travelling, can be related to the pseudorange between the satellite and the receiver. Hence we separate the carrier phase component from the complex amplitude in (4) and consider it as a function of the target dynamics.

Assuming that The positions of the M satellites, which are visible to the receiver at a given time instant, are given by $\boldsymbol{r}_i = (r_{x,i}, r_{y,i}, r_{z,i})^\top$, $i \in \{1, 2, \cdots, M\}$ and the real-value amplitude scalar of each transmission signal is denoted by α, the complete model of the received signal is

$$x(t) = \sum_{i=1}^{M} \alpha_i s(t - \tau_i(\boldsymbol{\kappa})) \exp\left(j2\pi f_{d,i}(\boldsymbol{\kappa})t\right) \exp\left(j\varphi_i(\boldsymbol{\kappa})\right) + n(t), \tag{9}$$

and we have

$$\begin{aligned} \tau_i(\boldsymbol{\kappa}) &= \frac{1}{c}||\boldsymbol{\theta} - \boldsymbol{r}_i|| + (\delta t - \delta t_i) \\ f_{d,i}(\boldsymbol{\kappa}) &= -(\boldsymbol{v}_i - \boldsymbol{v})^\top \boldsymbol{u}_i(\boldsymbol{\theta})(1 + \dot{\delta t})\frac{f_c}{c} \\ \varphi_i(\boldsymbol{\kappa}) &= 2\pi \frac{||\boldsymbol{\theta} - \boldsymbol{r}_i|| + c(\delta t - \delta t_i)}{\lambda}, \end{aligned} \tag{10}$$

where λ is the wavelength of the corresponding satellite signal band. The model of the carrier-phase φ_i comes from its physical meaning of how it shifts the phase of the signal. The models of delay τ and Doppler shift are reproducing the same model in (1) and (2) to clarify the above expression (9).

In order to implement DPE approach with real-world data record, we assume the receiver samples the signal at a fixed rate $f_s = 1/T_s$. The model can be rewritten in its discrete-time vector form equivalent as

$$x(kT_s) = \boldsymbol{\alpha}^\top \boldsymbol{\omega}_k(\boldsymbol{\kappa}) + n(kT_s), \tag{11}$$

where $\boldsymbol{\alpha} = [\alpha_1, \alpha_2, \cdots, \alpha_M]^\top \in \mathbb{R}^{M \times 1}$ is the real-value amplitude vector, $n(kT_s)$ denotes the sampled AWGN process and $\boldsymbol{\omega}_k(\boldsymbol{\kappa}) \in \mathbb{C}^{M \times 1}$ denotes the vector of the shifted PRN codes as shown in (12)

$$\boldsymbol{\omega}_k(\boldsymbol{\kappa}) = \begin{bmatrix} \omega_1(\boldsymbol{\kappa}) \\ \omega_2(\boldsymbol{\kappa}) \\ \vdots \\ \omega_M(\boldsymbol{\kappa}) \end{bmatrix} = \begin{bmatrix} s_1(\boldsymbol{\kappa}) d_1(\boldsymbol{\kappa}) \Phi_1(\boldsymbol{\kappa}) \\ s_2(\boldsymbol{\kappa}) d_2(\boldsymbol{\kappa}) \Phi_2(\boldsymbol{\kappa}) \\ \vdots \\ s_M(\boldsymbol{\kappa}) d_M(\boldsymbol{\kappa}) \Phi_M(\boldsymbol{\kappa}) \end{bmatrix}$$
$$= \begin{bmatrix} s_1(kT_s - \tau_1) \exp(j2\pi f_{d,1} k T_s) \exp(j\varphi_1) \\ s_2(kT_s - \tau_2) \exp(j2\pi f_{d,2} k T_s) \exp(j\varphi_2) \\ \vdots \\ s_M(kT_s - \tau_M) \exp(j2\pi f_{d,M} k T_s) \exp(j\varphi_M) \end{bmatrix}. \quad (12)$$

Supposing that total K samples are recorded in an observation window, forming the snapshot vector $\boldsymbol{x} = [x_1, x_2, \cdots, x_K]^\top \in \mathbb{C}^{K\times 1}$ with $x_k \triangleq x(kT_s)$, by maximizing the the log-likelihood function of the received signal given unknown parameter $\mathcal{L}(\boldsymbol{x}|\boldsymbol{\kappa})$, the estimator is given as

$$\begin{aligned} \hat{\boldsymbol{\kappa}} &= \arg\min_{\boldsymbol{\kappa}} J(\hat{\boldsymbol{\alpha}}, \boldsymbol{\kappa}) \\ &= \arg\max_{\boldsymbol{\kappa}} \Re\{\boldsymbol{x}^H \boldsymbol{\Omega}\} \Re\{\boldsymbol{\Omega}^H \boldsymbol{\Omega}\}^{-1} \Re\{\boldsymbol{x}^H \boldsymbol{\Omega}\}^\top, \end{aligned} \quad (13)$$

where $\Re\{\cdot\}$ denotes the real part of a complex value; and $\boldsymbol{\Omega} = (\boldsymbol{\omega}_1, \boldsymbol{\omega}_2, \cdots, \boldsymbol{\omega}_K)^\top \in \mathbb{C}^{K\times M}$ contains the samples of the local replica (the columns) of the M satellites (the rows).

Assuming that the processed signal in $\boldsymbol{x}$ is sampled at the chip rate from GPS L1 C/A signals, we can further simplify the estimator by making use of the approximation $\boldsymbol{\Omega}^H \boldsymbol{\Omega} \approx \boldsymbol{I}$ due to the desirable auto-correlation properties of the PRN codes used in GPS without secondary peaks in their auto-correlation function [5, Ch. 21]. In this case, we have

$$J_{\text{GPS}}(\hat{\boldsymbol{\alpha}}, \boldsymbol{\kappa}) = \boldsymbol{x}^H \boldsymbol{x} - \Re\{\boldsymbol{x}^H \boldsymbol{\Omega}\} \Re\{\boldsymbol{x}^H \boldsymbol{\Omega}\}^\top. \quad (14)$$

which leads to

$$\begin{aligned} \hat{\boldsymbol{\kappa}} &= \arg\min_{\boldsymbol{\kappa}} J_{\text{GPS}}(\hat{\boldsymbol{\alpha}}, \boldsymbol{\kappa}) \\ &= \arg\max_{\boldsymbol{\kappa}} \Re\{\boldsymbol{x}^H \boldsymbol{\Omega}\} \Re\{\boldsymbol{x}^H \boldsymbol{\Omega}\}^\top \\ &= \arg\max_{\boldsymbol{\kappa}} \sum_{i=1}^{M} \Re\{\boldsymbol{x}^H \bar{\boldsymbol{c}}_i(\boldsymbol{\kappa})\}^2 \\ &= \arg\max_{\boldsymbol{\kappa}} \Lambda_{\text{PDPE}}(\boldsymbol{a}, \boldsymbol{\kappa}), \end{aligned} \quad (15)$$

where $\bar{\boldsymbol{c}}_i$ is the local replica vector for the i-th satellite

$$\bar{\boldsymbol{c}}_i(\boldsymbol{\kappa}) = \begin{bmatrix} s_i(T_s - \tau_i) \exp(j2\pi f_{d,i} T_s) \exp(j\varphi_i) \\ s_i(2T_s - \tau_i) \exp(j2\pi f_{d,i} 2T_s) \exp(j\varphi_i) \\ \vdots \\ s_i(KT_s - \tau_i) \exp(j2\pi f_{d,i} K T_s) \exp(j\varphi_i) \end{bmatrix}, \quad (16)$$

which contrasts to the local replica $\boldsymbol{c}_i$, defined in (7) and used in DPE solution (5). In PDPE, $\bar{\boldsymbol{c}}_i$ is the i-th column of matrix $\boldsymbol{\Omega}$ containing the samples of the M local replicas. One should notice that this new estimator for PDPE takes the real part rather than the absolute value of the cost function.

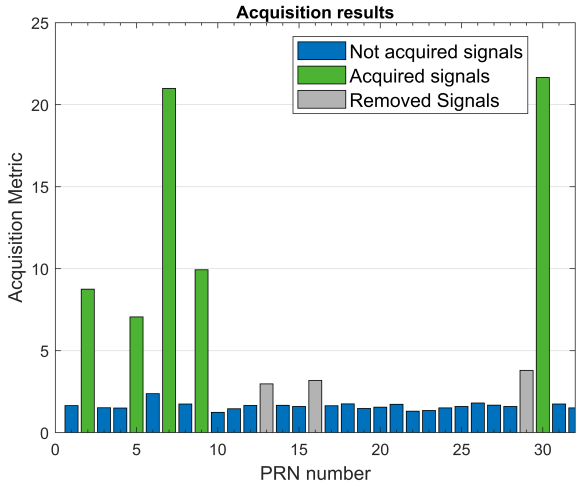

Fig. 2. Acquisition metric for the considered real-data experiment.

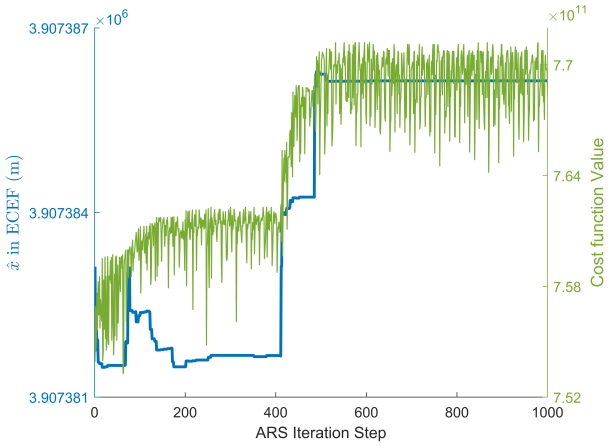

Fig. 3. Estimate of the x coordinate in ECEF and the associated cost function value during ARS iterations.

IV. Experimental Results

In recent years, the software-defined radio (SDR) paradigm has been rapidly developed for communication, data collection and signal processing fields. The SDR applications on GNSS receiver side has raised spread focus due to its simplified radio architectures, high flexibility of prototyping and low cost benefits [18], [19] (see [20] for a recent comprehensive review). SDR techniques enable one to collect the GNSS data with multi-receiver and multi-band, which can be processed with reconfigurable and reprogramming software online or offline [21]. For example, GNSS-SDR is developed as an open source GNSS software-defined receiver for positioning, navigation or any signal processing algorithms of interest [22]. To promote the interoperability of GNSS SDR data collections and processors, a metadata standard is created by ION for GNSS sampling data file decoding and encoding [23]. In a meanwhile, several such data files sampled from popular SDRs, e.g. HackerRF, LimeSDR, SiGe, USRP, etc., are re-

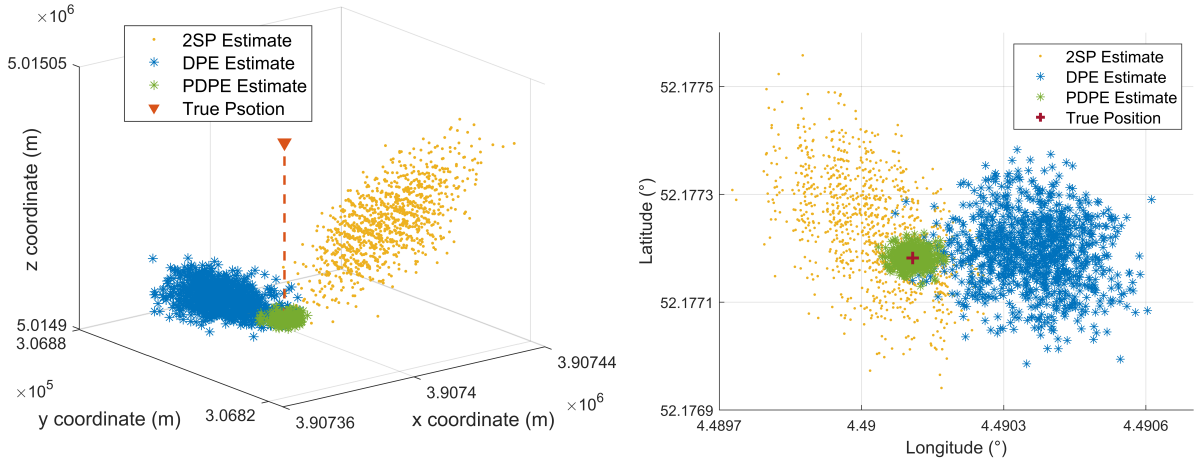

(a) ECEF Coordinate

(b) Latitude, Longitude and Altitude

Fig. 4. Position estimation result of 2SP, DPE and PDPE approaches in ECEF coordinate (left) and latitude, longitude and altitude system (right).

leased on https://sdr.ion.org/api-sample-data.html. The following experiments are implemented with the website dataset recored by LimeSDR, which is sampled at 10 MHz with 16 bit I/Q complex signal and 420 KHz intermediate frequency for GPS L1 signals. The dataset description indicates that total 8 GPS L1 signals with the PRN 2, 5, 6, 7, 9, 13, 29 and 30 are acquired, while we removed 3 of them due to relatively low acquisition metric (e.g. PRN 13, 16) and low elevation (e.g. PRN 29) as shown in Fig. 2.

A. Cross-Ambiguity Function

In this section, the CAFs of DPE and PDPE approach are plotted to help readers understand why the carrier phase, as a function of the receiver position, can improve the DPE positioning performance. Similarly as in [13], in order to visualize the cost function, only 2-dimensional position coordinates (θ_x, θ_y) are considered as unknown variables, while the other parameters in $\boldsymbol{\kappa}$ are fixed to their true values. For realization, we select the samples of an arbitrary one-millisecond sequence of raw signal recorded by the SDR.

The CAFs in Fig. 1 has been normalized by its maximum value. Both of the cost functions (DPE and PDPE) have one obvious peak when we observe the shape of the CAFs from 1 km range of the true location. However, within a smaller range, the shape of standard DPE cost function will soon become flat. When the range is zoomed within decimeter level, it is not likely to find a unique maximum point since some areas become completely flat. On the other hand, the carrier phase in PDPE brings high sensitivity of the cost function value to the estimate position. Hence, the cost function of PDPE is always able to fluctuate with the change of the receiver position estimate, which improves the precision of the DPE approach.

B. Estimation Result

It is intuitive to separate the estimation of the position and velocity of the target in the traditional state estimation problem. Hence this section will focus on estimation of the position-related parameters and consider velocity-related parameters as given or known variables. The 3-dimensional position in Earth-centered, Earth-fixed (ECEF) coordinate system and the clock bias of the receiver will be considered as 4 unknown variables $[\theta_x, \theta_y, \theta_z, \delta t]^\top \triangleq [\boldsymbol{\theta}^\top, \delta t]^\top$.

As discussed earlier, many useful optimization tools can be employed to solve the optimization problem in the ML estimator (5) and (15), which is equivalent to looking for the maximum point in Fig. 1. The gird search method can find the maximum by computing and comparing CAF values at all candidates of receiver position. However, due to the multivariate estimation and precision we expect to reach, it will cost huge data storage space and computation time. The extreme fluctuating shape of the PDPE CAF also prevents the utilization of gradient-based method. Hence, we exploit ARS method [17] to search the optimization solution for $[\boldsymbol{\theta}^\top, \delta t]^\top$, in which the consuming time can be limited by the fixed number of iterations and the precision can be controlled by the minimum search step. One should notice that the ARS parameter setting should enable the position search and the cost function value to converge. For example, when we set the maximum search step as 1 m and recursively search in 1000 iterations, the searching parameter and cost function value will converge under these settings as shown in figure 3. Although only the searching process of one coordinate is shown due to the plot restriction, the four variables in $[\boldsymbol{\theta}^\top, \delta t]^\top$ are searched simultaneously in iterations.

Fig. 4 shows the position estimation result of the receiver with 10000 ms recorded GNSS signal in ECEF coordinate and latitude, longitude and altitude system. The traditional 2SP method is exploited by the open-source GNSS-SDR [6], [22] as a benchmark. The receiver processes and tracks the signal every 10 ms so that total 1000 times of estimation is generated. DPE and PDPE are implemented by ARS based on a sequence of one-millisecond GNSS signal samples every 10 ms. Thus

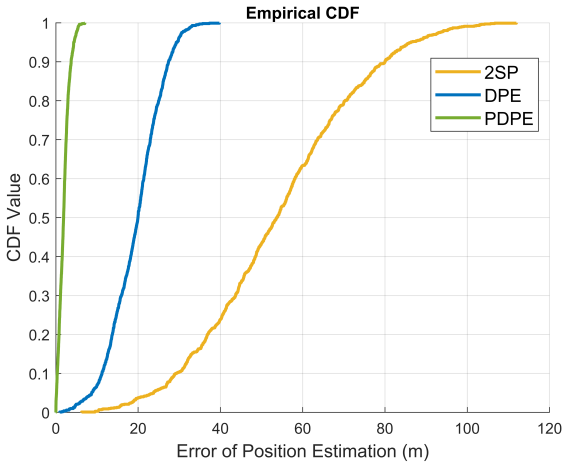

Fig. 5. Empirical CDF of position estimation error.

1000 times of estimation are computed corresponding to the same time stamp of 2SP method. To clarify the positioning performance, Fig. 5 shows empirical cumulative distribution function (CDF) of the position estimation error based on the result in Fig. 4. From the cloud points gathering pattern in Fig. 4 and the error distribution in Fig. 5, one can find that the proposed PDPE approach outperforms DPE, and consequently 2SP method as well, in the terms of less bias and more precision.

V. Conclusions

This paper proposed a novel GNSS direct-positioning approach, termed Precise DPE (PDPE), which extends the existing DPE framework by relating the carrier-phase to the receiver dynamics. This brings a new maximum likelihood estimator of the position parameter, which not only brings the high-sensitivity benefits that DPE had but also increased precision brought by employing the carrier-phase variable. Another contribution of this paper is to present, the first implementation of PDPE on real data and its comparison to DPE and two-steps solutions. The methods were implemented on a software-defined radio platform and the associated implementation aspects were addressed. The experiments show that the PDPE performs better than the standard DPE in terms of both precision and accuracy, and as expected it outperforms traditional two-step methodologies.

References

[1] E. D. Kaplan and C. Hegarty, *Understanding GPS/GNSS: principles and applications*. Artech house, 2017.

[2] B. Hofmann-Wellenhof, H. Lichtenegger, and E. Wasle, *GNSS–global navigation satellite systems: GPS, GLONASS, Galileo, and more*. Springer Science & Business Media, 2007.

[3] T. Pany, *Navigation signal processing for GNSS software receivers*. Artech House, 2010.

[4] P. J. Teunissen and O. Montenbruck, *Springer handbook of global navigation satellite systems*. Springer, 2017, vol. 10.

[5] Y. J. Morton, F. van Diggelen, J. J. Spilker Jr, B. W. Parkinson, S. Lo, and G. Gao, *Position, Navigation, and Timing Technologies in the 21st Century: Integrated Satellite Navigation, Sensor Systems, and Civil Applications*. John Wiley & Sons, 2021.

[6] K. Borre, D. M. Akos, N. Bertelsen, P. Rinder, and S. H. Jensen, *A software-defined GPS and Galileo receiver: a single-frequency approach*. Springer Science & Business Media, 2007.

[7] R. T. Ioannides, T. Pany, and G. Gibbons, "Known vulnerabilities of global navigation satellite systems, status, and potential mitigation techniques," *Proceedings of the IEEE*, vol. 104, no. 6, pp. 1174–1194, 2016.

[8] M. G. Amin, P. Closas, A. Broumandan, and J. L. Volakis, "Vulnerabilities, threats, and authentication in satellite-based navigation systems," *Proceedings of the IEEE*, vol. 104, no. 6, pp. 1169–1173, 2016.

[9] M. Petovello, C. O'Driscoll, and G. Lachapelle, "Weak signal carrier tracking using extended coherent integration with an ultra-tight gnss/imu receiver," in *European Navigation Conference*, 2008, pp. 23–25.

[10] A. Amar and A. J. Weiss, "New asymptotic results on two fundamental approaches to mobile terminal location," in *2008 3rd International Symposium on Communications, Control and Signal Processing*. IEEE, 2008, pp. 1320–1323.

[11] P. Closas, C. Fernández-Prades, and J. A. Fernández-Rubio, "Direct position estimation approach outperforms conventional two-steps positioning," in *2009 17th European Signal Processing Conference*. IEEE, 2009, pp. 1958–1962.

[12] A. Gusi-Amigó, P. Closas, A. Mallat, and L. Vandendorpe, "Cramér-rao bound analysis of UWB based localization approaches," in *2014 IEEE International Conference on Ultra-WideBand (ICUWB)*. IEEE, 2014, pp. 13–18.

[13] P. Closas and A. Gusi-Amigó, "Direct position estimation of GNSS receivers: Analyzing main results, architectures, enhancements, and challenges," *IEEE Signal Processing Magazine*, vol. 34, no. 5, pp. 72–84, 2017.

[14] A. Gusi-Amigó, P. Closas, A. Mallat, and L. Vandendorpe, "Ziv-Zakai bound for direct position estimation," *NAVIGATION, Journal of the Institute of Navigation*, vol. 65, no. 3, pp. 463–475, 2018.

[15] P. Closas, C. Fernández-Prades, and J. A. Fernández-Rubio, "Maximum likelihood estimation of position in GNSS," *IEEE Signal Processing Letters*, vol. 14, no. 5, pp. 359–362, 2007.

[16] M. Peretic and G. X. Gao, "Design of a parallelized direct position estimation-based GNSS receiver," *NAVIGATION: Journal of the Institute of Navigation*, vol. 68, no. 1, pp. 21–39, 2021.

[17] M. Appel, R. Labarre, and D. Radulovic, "On accelerated random search," *SIAM Journal on Optimization*, vol. 14, no. 3, pp. 708–731, 2004.

[18] J.-H. Won, T. Pany, and G. W. HeiN, "Gnss software defined radio," *Inside GNSS*, vol. 1, no. 5, pp. 48–56, 2006.

[19] L. L. Presti, P. di Torino, E. Falletti, M. Nicola, and M. T. Gamba, "Software defined radio technology for gnss receivers," in *2014 IEEE Metrology for Aerospace (MetroAeroSpace)*. IEEE, 2014, pp. 314–319.

[20] D. Akos, J. Arribas, M. Z. H. Bhuiyan, P. Closas, F. Dovis, I. Fernandez-Hernandez, C. Fernández-Prades, S. Gunawardena, T. Humphreys, Z. M. Kassas *et al.*, "GNSS Software Defined Radio: History, Current Developments, and Standardization Efforts," in *Proceedings of the 35th International Technical Meeting of the Satellite Division of The Institute of Navigation (ION GNSS+ 2022)*, 2022, pp. 3180–3209.

[21] F. Principe, G. Bacci, F. Giannetti, and M. Luise, "Software-defined radio technologies for gnss receivers: A tutorial approach to a simple design and implementation," *International Journal of Navigation and Observation*, vol. 2011, 2011.

[22] C. Fernandez-Prades, J. Arribas, P. Closas, C. Aviles, and L. Esteve, "GNSS-SDR: An open source tool for researchers and developers," in *Proceedings of the 24th International Technical Meeting of The Satellite Division of the Institute of Navigation (ION GNSS 2011)*, 2011, pp. 780–794.

[23] S. Gunawardena, T. Pany, and J. Curran, "Ion gnss software-defined radio metadata standard," *NAVIGATION: Journal of the Institute of Navigation*, vol. 68, no. 1, pp. 11–20, 2021.